Received: 25 July 2018 | Revised: 21 November 2018 | Accepted: 21 December 2018

DOI: 10.1111/ejn.14334

SPECIAL ISSUE ARTICLE

WILEY EJN European Journal of Neuroscience FENS

Circadian rhythm of redox state regulates membrane excitability in hippocampal CA1 neurons

Ghazal Naseri Kouzehgarani[1,2,*] | **Mia Y. Bothwell**[3,*] | **Martha U. Gillette**[1,2,3,4]

[1]Neuroscience Program, University of Illinois at Urbana-Champaign, Urbana, Illinois

[2]Beckman Institute for Advanced Science & Technology, University of Illinois at Urbana-Champaign, Urbana, Illinois

[3]Department of Molecular & Integrative Physiology, University of Illinois at Urbana-Champaign, Urbana, Illinois

[4]Department of Cell & Developmental Biology, University of Illinois at Urbana-Champaign, Urbana, Illinois

Correspondence
Martha U. Gillette, Neuroscience Program, Departments of Cell & Developmental Biology and Molecular & Integrative Physiology, Beckman Institute for Advanced Science & Technology, University of Illinois at Urbana-Champaign, Urbana, IL.
Email: mgillett@illinois.edu

Funding information
National Science Foundation, Division of Graduate Education, Grant/Award Number: IGERT CMMB 0965918; Medical Scholars Program, University of Illinois; National Science Foundation, Division of Chemical, Bioengineering, Environmental, and Transport Systems, Grant/Award Number: STC EBICS 0939511; National Science Foundation, Division of Integrative Organismal Systems, Grant/Award Number: IOS 1354913; Beckman Institute Graduate Fellows Program, University of Illinois; National Institute of Mental Health, Grant/Award Number: MH 109062

Abstract

Behaviors, such as sleeping, foraging, and learning, are controlled by different regions of the rat brain, yet they occur rhythmically over the course of day and night. They are aligned adaptively with the day-night cycle by an endogenous circadian clock in the suprachiasmatic nucleus (SCN), but local mechanisms of rhythmic control are not established. The SCN expresses a ~24-hr oscillation in reduction-oxidation that modulates its own neuronal excitability. Could circadian redox oscillations control neuronal excitability elsewhere in the brain? We focused on the CA1 region of the rat hippocampus, which is known for integrating information as memories and where clock gene expression undergoes a circadian oscillation that is in anti-phase to the SCN. Evaluating long-term imaging of endogenous redox couples and biochemical determination of glutathiolation levels, we observed oscillations with a ~24 hr period that is 180° out-of-phase to the SCN. Excitability of CA1 pyramidal neurons, primary hippocampal projection neurons, also exhibits a rhythm in resting membrane potential that is circadian time-dependent and opposite from that of the SCN. The reducing reagent glutathione rapidly and reversibly depolarized the resting membrane potential of CA1 neurons; the magnitude is time-of-day-dependent and, again, opposite from the SCN. These findings extend circadian redox regulation of neuronal excitability from the SCN to the hippocampus. Insights into this system contribute to understanding hippocampal circadian processes, such as learning and memory, seizure susceptibility, and memory loss with aging.

KEYWORDS

CA1 pyramidal neurons, circadian clock, rat hippocampus, reduction-oxidation, suprachiasmatic nucleus

Abbreviations: ACSF, artificial cerebrospinal fluid; BioGEE, biotinylated glutathione ethyl ester; CREB, Ca^{2+}/cAMP response element-binding protein; CT, circadian time; DAB, 3,3-diaminobenzidine; EBSS, essential balanced salt solution; FAD, flavin adenine dinucleotide; GSH, glutathione; GSH-Px, glutathione peroxidase; GSK3, glycogen synthase kinase 3; GSK3β, glycogen synthase kinase 3-beta; GSSG, glutathione disulfide; I-V, current-voltage; L/D, light/dark; LTP, long-term potentiation; MAPK, cAMP/mitogen-activated protein kinase; NAD^+/NADH, nicotinamide adenine dinucleotide (oxidized/reduced); $NADP^+$/NADPH, nicotinamide adenine dinucleotide phosphate (oxidized/reduced); Rin, input resistance; ROI, region of interest; SCN, suprachiasmatic nucleus; TTX, tetrodotoxin; Vm, membrane potential; ZT, zeitgeber time; τ, *tau*, endogenous circadian period.

[*]These authors contributed equally to the manuscript.

Edited by Rae Silver. Reviewed by Akhilesh Reddy and John O'Neill.

All peer review communications can be found with the online version of the article.

1 | INTRODUCTION

The suprachiasmatic nucleus (SCN), the master clock oscillator, regulates multiple aspects of metabolic homeostasis, including the levels of many circulating metabolites, liver enzymes and hormones, daily fluctuations in energy production and utilization, and fasting/feeding behavior (Bass & Takahashi, 2010; Green, Takahashi, & Bass, 2008). The relationship between metabolism and circadian rhythms is thought to be of a complex, reciprocal nature, in that the SCN regulates metabolic activity and in turn is affected by metabolic signaling pathways (Rutter, Reick, & McKnight, 2002).

Cellular energy metabolism is linked to redox homeostasis (Griffiths, Gao, & Pararasa, 2017). The redox environment of a tissue is defined by the balance of oxidizing and reducing potentials of all available redox-molecule pairs. Redox state, an indicator of the redox environment, is measured as the ratio of the oxidized to the reduced form of a specific redox couple, such as nicotinamide adenine dinucleotide (NAD^+)/reduced NAD^+ (NADH), $NADP^+$/NADPH, or glutathione disulfide (GSSG)/glutathione (GSH) (Dröge, 2002; Schafer & Buettner, 2001).

The redox environment and circadian rhythms are coupled through the transcriptional-translational modulation of the core clock genes in the SCN. The redox oscillation requires functionally intact clock machinery, and clock gene expression is sensitive to changes in cellular metabolism (Bass & Takahashi, 2010; Green et al., 2008; Rutter et al., 2002). The non-transcriptional interdependency of redox state and circadian rhythm in the central clock has been investigated by Wang et al. (2012). An intrinsic, self-sustained circadian oscillation in SCN redox couples was detected. That novel study also found that redox oscillation could regulate SCN neuronal excitability through non-transcriptional modulation of K^+ channels (Gillette & Wang, 2014; Wang et al., 2012).

Several extra-SCN oscillators have been identified in the central nervous system that are synchronized by the SCN. Robust rhythms in expression of core clock genes and electrical activity are observed in a number of structures, such as other hypothalamic nuclei, the olfactory bulb, amygdala, cerebellum, cerebral cortex, and hippocampus (Abe et al., 2002; Granados-Fuentes, Prolo, Abraham, & Herzog, 2004; Guilding & Piggins, 2007). The hippocampus is of interest due to its importance in learning and memory. Rhythmic expressions of *Per1* and *Per2* have been found in the CA1, CA2, CA3, and dentate gyrus regions of the hippocampus (Feillet, Mendoza, Albrecht, Pévet, & Challet, 2008; Wakamatsu et al., 2001; Wang et al., 2009). Strikingly, hippocampal clock gene rhythms are in anti-phase to those in the SCN (Wang et al., 2009).

Accumulating evidence suggests that hippocampal function and susceptibility to dysfunction display circadian rhythmicity. A landmark study demonstrated that memory retention after associative learning oscillates in a circadian manner. (Holloway & Wansley, 1973). This oscillatory pattern was not present in SCN-lesioned animals with severely disrupted circadian rhythms (Stephan & Kovacevic, 1978). Since then, numerous other studies in rats and humans have shown that phase shifts and disturbances in circadian rhythmicity interfere with hippocampus-dependent memory formation and consolidation (Cho, Ennaceur, Cole, & Suh, 2000; Fekete, van Ree, Niesink, & de Wied, 1985; Tapp & Holloway, 1981). Importantly, hippocampal memory acquisition, learning, and performance of recalled behavioral tasks require a functionally intact circadian system (Ruby et al., 2008; Wright, Hull, Hughes, Ronda, & Czeisler, 2006).

Hippocampal long-term potentiation (LTP) is a form of experience-induced functional change in which synaptic connections undergo activity-dependent changes in synaptic strength. *Per2*-mutant mice exhibit abnormal LTP, suggesting a functional dependency (Wang et al., 2009). Day/night rhythms in LTP in the rodent hippocampus have been reported with potentiation of greater magnitude in the nighttime (Chaudhury & Colwell, 2002; Harris & Teyler, 1983). These studies were performed in brain slices trimmed to remove extra-hippocampal structures. These diurnal variations were maintained under a 12:12 hr light/dark (L/D) schedule as well as in constant darkness and were not dependent on the time of brain slice preparation (Chaudhury, Wang, & Colwell, 2005). These studies suggest that this functional change may be under endogenous circadian control.

Pathways of memory consolidation may need to be activated repeatedly to be most effective. The presence of common diurnal variations in the hippocampus and SCN as well as strong evidence implicating circadian rhythmicity in memory formation suggest that there may be other shared links. Therefore, we hypothesized that extra-SCN brain regions, such as the hippocampus, may exhibit diurnal oscillations in redox state that regulate day-night differences in neuronal function (Bothwell & Gillette, 2018). In this study, we report that the hippocampal CA1 region undergoes a near-24-hr redox oscillation that is anti-phase to that of the SCN. We provide evidence that, like the SCN, the hippocampus exhibits circadian oscillations in both membrane excitability and redox state that could play roles in modulating time-of-day differences in the integrative capacity of hippocampal CA1 pyramidal neurons during memory formation.

2 | MATERIALS AND METHODS

2.1 | Animals

Long-Evans/BluGill rats (total of 63 animals, 30F and 33M) were used for immunohistochemistry (three animals, all M),

real-time redox imaging (one animal, M), glutathiolation assay (24 animals, 12F and 12M), endogenous biotin measurement (five animals, all M), and patch-clamp recording (30 animals, 18F and 12M). Breeding colonies were generated and maintained at the University of Illinois at Urbana-Champaign (UIUC). Animals were housed under standard conditions on a 12:12 hr L/D schedule and given food and water ad libitum. All experimental animals were rapidly decapitated using a guillotine, without anesthesia or sedatives, to avoid shifting the endogenous circadian clock (Gillette, 1985). All experimental protocols were in compliance with the National Institutes of Health Public Health Service Policy on Humane Care and Use of Laboratory Animals and were approved by the UIUC Institutional Animal Care and Use Committee.

2.2 | Immunohistochemistry

Coronal brain slices (500 μm-thick) of the hippocampus and the ventromedial hypothalamus containing the SCN were prepared separately from 6 to 8-week-old animals on a mechanical tissue chopper. The hippocampus was isolated with a scalpel, and the SCN region was isolated with a 2 mm diameter tissue punch. Brain slices were maintained in a tissue chamber perfused with Earle's Essential Balanced Salt Solution (EBSS) (NaCl 116.4 mM, KCl 5.4 mM, $CaCl_2$ 1.8 mM, $MgSO_4$ 0.8 mM, NaH_2PO_4 1.0 mM, glucose 24.5 mM, $NaHCO_3$ 26.2 mM, gentamicin 1 mg/L, pH 7.2–7.4, 290–300 mOsm/L) saturated with 95% O_2/5% CO_2 at 37°C. Tissue slices were incubated with 250 μM biotinylated glutathione ethyl ester (BioGEE, Invitrogen, Carlsbad, CA, USA), a biotin amide that binds to and permits imaging of sulfhydryl groups in proteins. Incubation was done for 1 hr before collection at circadian times (CT) 6 and 14 and fixed in 4% paraformaldehyde for 2 hr. Tissue was then sliced at 20 μm on the cryostat and mounted on glass slides. Slices were pre-treated with 1% H_2O_2 in PBS for 30 min, followed by incubation with Avidin/Biotin-Horse Radish Peroxidase (ABC-HRP) reagent (Vector Labs, Burlingame, CA, USA) according to the manufacturer's instructions for 1 hr. Following this incubation, tissue slices were washed in PBS and 175 mM sodium acetate. Slices were then developed in a 3,3′-diaminobenzidine (DAB) solution (85 mM sodium acetate, 320 μM $NiSO_4$, 0.01% DAB) for 20 min. Controls for endogenous biotin consisted of identical brain slices not incubated with BioGEE.

For analysis, DAB-stained images were imported into ImageJ software (ImageJ, NIH, USA). Regions of interest (ROIs) were drawn around the SCN (300 × 300 μm) and the CA1 layer of the hippocampus (500 × 100 μm). Average pixel intensity was calculated for each ROI and divided by its respective area. The resulting value was then divided by the value from the control region of the same brain. Staining controls for the SCN and the hippocampus were the third ventricle and image background, respectively; neither control intensity changed with respect to time-of-day. The ROIs for the third ventricle were 50 × 50 μm. The ROIs for the hippocampal background were the same size as the CA1 ROIs. These normalized values enabled normalization for staining variances across brains.

2.3 | Brain slice preparation for intrinsic redox imaging

Hippocampal brain slices were prepared from 2 to 3-week-old rats between zeitgeber time (ZT) 6–9 (where ZT 0 = light onset and ZT 12 = light offset). The brain was quickly removed and immediately placed into an ice-cold slicing solution (KCl 2.5 mM, $MgSO_4$ 10.0 mM, $CaCl_2$ 0.5 mM, NaH_2PO_4 1.2 mM, glucose 11.0 mM, sucrose 234.0 mM, $NaHCO_3$ 26.2 mM, pH 7.2–7.4, 290–300 mOsm/L) saturated with 95% O_2/5% CO_2. A 350 μm-thick coronal hippocampal slice was cut using a vibrating blade microtome (Leica, Wetzlar, DE, USA) and transferred to a Millicell tissue culture insert (Millipore, Billerica, MA, USA) with Dulbecco's Modified Eagle Medium (DMEM) (Gibco, Carlsbad, CA, USA) containing 0.5% B-27 supplement, 1.0 mM glutamine, and 25 μg/ml penicillin/streptomycin at 37°C. Medium was changed the next day and slices were imaged after 2 days in culture.

2.4 | Real-time redox imaging

A hippocampal slice cultured for 2 days was transferred to a 37°C chamber on the microscope stage and perfused continuously with EBSS without phenol red saturated with 95% O_2/5% CO_2. Two-photon microscopy was performed with the Zeiss LSM 510 confocal laser-scanning microscope with MaiTai laser on a 20 × 0.8 NA objective (Carl Zeiss). Excitation wavelength was set to 730 nm and two channels of emission at 430–500 and 500–550 nm were recorded simultaneously (Georgakoudi & Quinn, 2012). Imaging sessions began at CT 9–11 with a sampling rate of 4 s/frame at 365 s intervals for 720 frames (72 hr total). Florescence intensity at 400+ nm (maximum NAD(P)H emission) and 500+ nm (maximum flavin adenine dinucleotide (FAD) emission) for each frame was acquired by Zeiss LSM software. Relative redox state was calculated from the ratio of fluorescence at 500+ nm over 400+ nm (F_{500+}/F_{400+}).

2.5 | Glutathiolation assay and endogenous biotin measurement

Coronal brain slices (500 μm-thick) of the hippocampus and the hypothalamus containing the SCN were prepared separately from 6 to 8-week-old animals as described above in the immunohistochemistry section. The brain slices were maintained in a tissue chamber perfused with EBSS saturated with 95% O_2/5%

CO_2 at 37°C. Tissue slices were either incubated with 250 μM BioGEE for 1 hr before collection for glutathiolation assay or remained in EBSS for evaluation of endogenous biotin levels. All samples were collected immediately post-treatment, flash-frozen on dry ice, and stored at −80°C until processing.

Each frozen sample was mixed with 200 μL RIPA buffer (50 mM Tris pH 7.5, 150 mM NaCl, 1 mM EDTA, 0.2% SDS, 1% NP-40, 0.5% sodium deoxycholate) with 1× cOmplete protease inhibitor cocktail (Roche, Basel, SUI) on ice and mechanically homogenized. After a 2-min incubation on ice, samples were centrifuged at 14,000 rpm and the supernatant was transferred to a clean tube. Protein concentration was determined by BCA protein assay (Pierce, Rockford, IL, USA). Total protein (25 μg/sample) was resolved in 8% SDS-PAGE and transferred to nitrocellulose membrane (Bio-Rad, Hercules, CA, USA). Membranes were probed with 1:2000 mouse anti-biotin peroxidase antibody (Cell signaling, Danvers, MA, USA) overnight and developed with SuperSignal chemiluminescent substrate (Pierce, Rockford, IL, USA). Blots were stripped with Restore Western Blot Stripping Buffer (Thermo Fisher Scientific, Rockford, IL, USA) and re-probed with anti-α-tubulin antibody (Cellsignaling, Danvers, MA, USA). Level of BioGEE incorporation was determined by the ratio of overall biotin intensity over the band intensity of the tubulin loading control and normalized to the maximum value of the same blot. Level of endogenous biotin was quantified by the overall intensity of the entire lane over the band intensity of tubulin.

2.6 | Patch-clamp recording

Animals for patch-clamp recording were 2 to 4 weeks old, and killed between ZT 0–12, depending on the time of the experiment. The brain was quickly removed and placed into an ice-cold slicing solution (KCl 2.5 mM, $MgSO_4$ 10.0 mM, $CaCl_2$ 0.5 mM, NaH_2PO_4 1.25 mM, $NaHCO_3$ 26.0 mM, glucose 11.0 mM, sucrose 234.0 mM) saturated with 95% O_2/5% CO_2. A 350 μm-thick coronal hippocampal brain slice was cut on a vibrating tissue slicer. Brain slices were then placed into a holding chamber containing artificial cerebrospinal fluid (ACSF) (NaCl 126.0 mM, KCl 2.5 mM, $MgCl_2$ 2.0 mM, $CaCl_2$ 2.0 mM, NaH_2PO_4 1.25 mM, $NaHCO_3$ 26.0 mM, glucose 10.0 mM, 300 mOsm/L) saturated with 95% O_2/5% CO_2 at room temperature. The slices were incubated between 1–9 hr before recording commenced.

Intracellular recordings of hippocampal CA1 pyramidal neurons, using the whole-cell patch-clamp technique, were obtained by electrodes with pipette-tip resistances of 4–7 MΩ. These microelectrodes were filled with an intracellular solution (K-gluconate 117 mM, KCl 13 mM, $MgCl_2$ 1.0 mM, $CaCl_2$ 0.07 mM, EGTA 0.1 mM, HEPES 10.0 mM, Na-ATP 2.0 mM, Na-GTP 0.4 mM, pH 7.3, 290 mOsm/L). A Multiclamp 700B amplifier was used for current-clamp recordings. Data were stored on computer for further analyses using the pClamp software (Molecular Devices, San Jose, CA, USA). Only neurons with initial access resistances ranging from 10 to 25 MΩ and remaining stable throughout the recording were included in analysis.

Under current-clamp mode, the membrane potential (Vm) of hippocampal CA1 pyramidal neurons was recorded at different CTs. The input resistance (Rin) of the same population of cells was measured in two ways: (a) from the linear slope of the current-voltage (I-V) curve obtained by applying a current-step protocol (duration 600 ms) from −100 pA to +200 pA with 20 pA increments, to assess the initial resistance of the cell at the beginning of recording, and (b) from the changes in the membrane potential response to a hyperpolarizing current injection, in order to assess the health of the neuron and the stability of the patch throughout the recording. Based on the pattern of action potential firing and the I-V curve, only pyramidal neurons were included in analysis and all other cell types were excluded from the pool of data.

The reducing reagent, glutathione (GSH, 1 mM, MilliporeSigma) was bath applied for 5 min to 63/112 of the current-clamped CA1 pyramidal neurons at different CTs and the change in Vm (ΔVm) was recorded. In order to prevent secondary effects from synaptic excitation, the entire experiment was carried out in the presence of tetrodotoxin (TTX, 0.5 μM, Tocris Bioscience, Minneapolis, MN, USA), a voltage-gated Na^+ channel blocker. Only neurons with Vm back to baseline post-GSH wash-out were kept for analysis.

2.7 | Statistical analysis

Statistical analysis was performed using SAS statistical software (SAS Studio, SAS Institute Inc., Cary, NC, USA). This software reports exact *p*-values except for when $p < 0.0001$. All data are presented as mean ± SEM. Due to the nature of DAB intensity values representing multiple slices/animal/time point, a two-way mixed-model ANOVA was used with Tukey's *post-hoc* comparison. The fixed, between-subject factors were brain region with two levels: the hippocampus and SCN, and time-of-day with two levels: CT 6 and CT 14. The random, within-subject factor was the individual animal to account for the correlation between the multiple slices within each individual. For analysis of endogenous biotin, student's unpaired *t* test was used. For all analyses of Vm, Rin, ΔVm, and glutathiolation assay, multiple comparisons were made using one-way ANOVA followed by the Tukey's post-hoc test. *p*-values < 0.05 were considered statistically significant. For analysis of real-time redox imaging, chi-square periodogram analysis was performed with a MATLAB toolbox, Clocklab (Version 5.3.1, Actimetrics, Wilmette, IL, USA), to determine the length of circadian period (τ). Chi-square values were calculated from recording data, and τ was determined from the highest value above confidence interval of 0.001.

3 | RESULTS

3.1 | Redox rhythm of the hippocampal CA1 layer is anti-phase to that of the SCN

To compare the relative redox states of the hippocampus and SCN, we obtained hippocampal and SCN tissues from the same animal and visualized biotinylated reduced glutathione (BioGEE) incorporation in mid-day (CT 6) and early night (CT 14). We found statistically significant differences, with BioGEE incorporation in the SCN low at CT 6 vs. high at CT 14 ($t_8 = 4.15$, $p = 0.01$), reflecting a reduced state in daytime and an oxidized state at nighttime. Conversely, BioGEE incorporation in the hippocampal CA1 layer was high at CT 6 vs. low at CT 14 ($t_8 = 2.99$, $p = 0.03$), indicating the hippocampus is more oxidized during the day and more reduced during the night. (Figure 1c, two-way mixed-model ANOVA with Tukey's post-hoc test, interaction between brain region and time of day: $F_{1,8} = 13.21$, $p = 0.006$, $n = 3$).

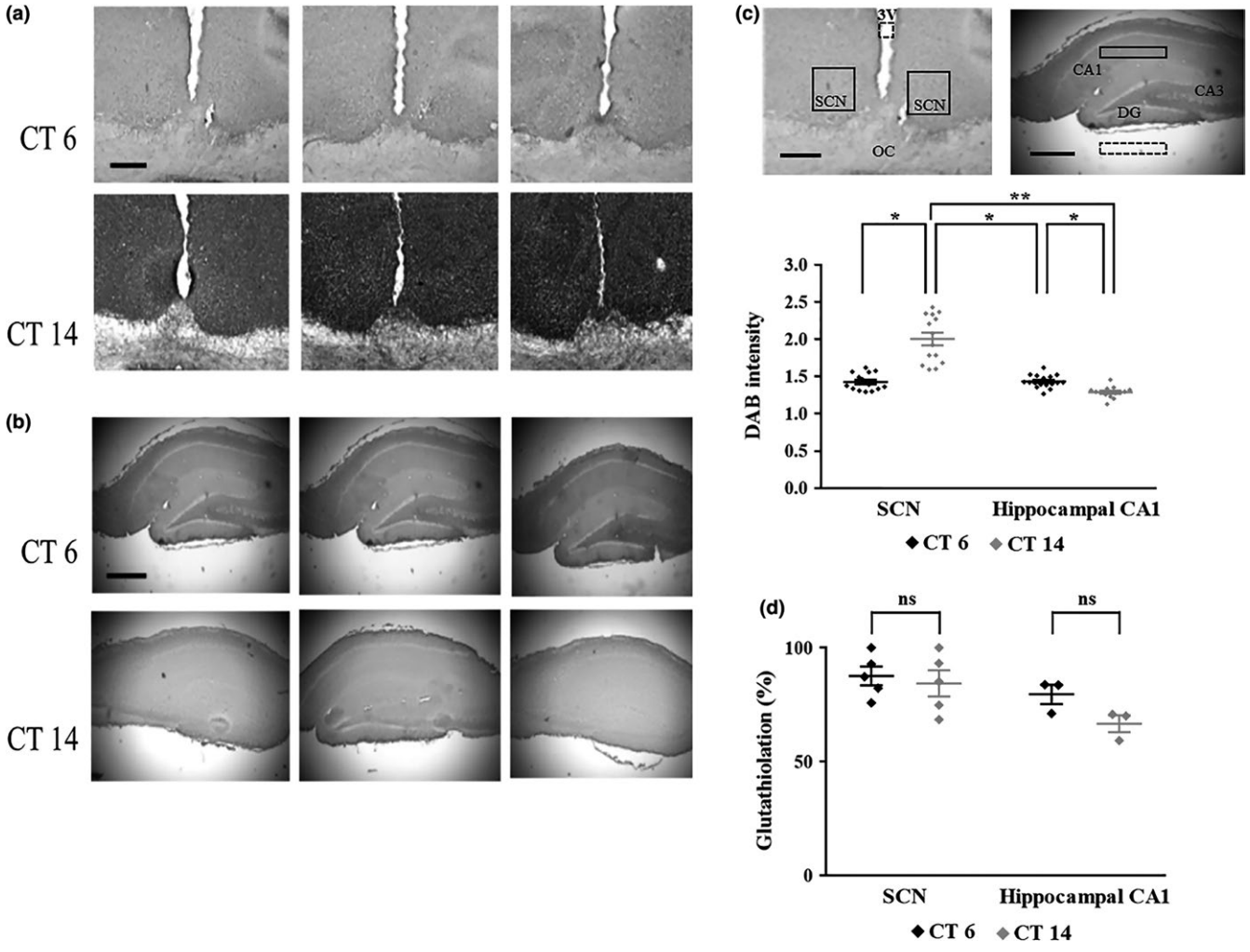

FIGURE 1 The hippocampal CA1 region and the SCN of the same animal exhibit opposite redox states in day vs. night. During the subjective day (CT 6), the SCN is more reduced and the CA1 is more oxidized, while during the subjective night (CT 14) the SCN is more oxidized and the CA1 is more reduced. (a) The SCN shows low BioGEE incorporation at CT 6 compared with high BioGEE incorporation at CT 14, reflecting a reduced state at CT 6 and oxidized state at CT 14. Scale bar = 500 μm. (b) Conversely, the hippocampal CA1 area shows high BioGEE incorporation at CT 6 and low BioGEE incorporation at CT 14, reflecting an oxidized state at CT 6 and reduced state at CT 14. Scale bar = 500 μm. (c) The intensity of DAB staining of BioGEE was measured using ImageJ. Representative images from CT 6 are shown with regions of interest (ROIs) around the SCN and the hippocampal CA1 layer (solid line) and control regions (dashed line). DAB staining intensity in the SCN is significantly higher at CT 14 vs. CT 6 ($p = 0.01$), but in the CA1 layer of hippocampus, staining is higher at CT 6 vs. CT 14 ($p = 0.03$). DAB intensity levels were significantly lower in the hippocampal CA1 region at CT 6 and CT 14 vs. the SCN at CT 14 ($p = 0.01$ and 0.004, respectively). Two-way mixed-model ANOVA; Tukey's post-hoc test. $^*p < 0.05$, $^{**}p < 0.01$, $n = 3$. 3V = 3rd Ventricle, OC = Optic Chiasm. Scale bar = 500 μm. (d) Quantification of western blots for comparison of endogenous biotin in rat SCN and hippocampal slices incubated with EBSS at CT 6 and CT 14 showed no statistically significant differences between the two time points (SCN: CT 6 (87.64 ± 4.18%) vs. CT 14 (84.32 ± 5.78%), $p = 0.65$; hippocampus: CT 6 (79.50 ± 4.19%) vs. CT 14 (66.63 ± 3.72%), $p = 0.08$). Student's unpaired t test, $n = 3$–5. ns: non-significant. Error bars represent SEM

In order to exclude the null hypothesis that a variation in endogenous biotin – rather than protein glutathiolation – is being observed, control western blots of brain slices incubated with EBSS and without BioGEE were performed (Supporting information Figure S1). Quantification of western blots for comparison of endogenous biotin in rat SCN slices at CT 6 (87.64 ± 4.18%) and CT 14 (84.32 ± 5.78%) showed no statistically significant differences between the two time points. Additionally, quantification of endogenous biotin in rat hippocampal slices at CT 6 (79.50 ± 4.19%) and CT 14 (66.63 ± 3.72%) displayed no statistically significant day/night differences (Figure 1d, Student's unpaired *t* test; $t_8 = 0.47$, $p = 0.65$, $n = 5$; $t_4 = 2.29$, $p = 0.08$, $n = 3$, respectively).

3.2 | Redox state undergoes an endogenous oscillation in the rat hippocampal CA1 layer

Using real-time ratiometric redox imaging of auto-fluorescent metabolic cofactors FAD and NAD(P)H, we found a near-24-hr oscillation of redox state in the CA1 region of the rat hippocampus. The coronal hippocampal slice was first cultured for 2 days and then imaged for 3 days. The redox oscillation persisted throughout all 3 days of imaging. Chi-square periodogram analysis revealed that the period, $\tau = 22.75$ hr (Figure 2).

3.3 | CA1 pyramidal neurons display distinctive morphological and electrophysiological properties

To evaluate possible relationships between the circadian oscillation of redox state and neuronal physiology, whole-cell patch-clamp recordings were obtained from CA1 pyramidal neurons in the rat hippocampal CA1 region. Hippocampal CA1 pyramidal neurons filled with Alexa Fluor 488 dye (Thermo Fisher Scientific, Rockford, IL, USA) via patch electrode have a distinctive dendritic morphology (Figure 3a,b). Voltage response to current steps (I-V curve) with duration of 600 ms ranging from −100 to +200 pA with 20 pA increments, exhibited the characteristic pattern of action potential firing of hippocampal CA1 neurons, with peak depolarization

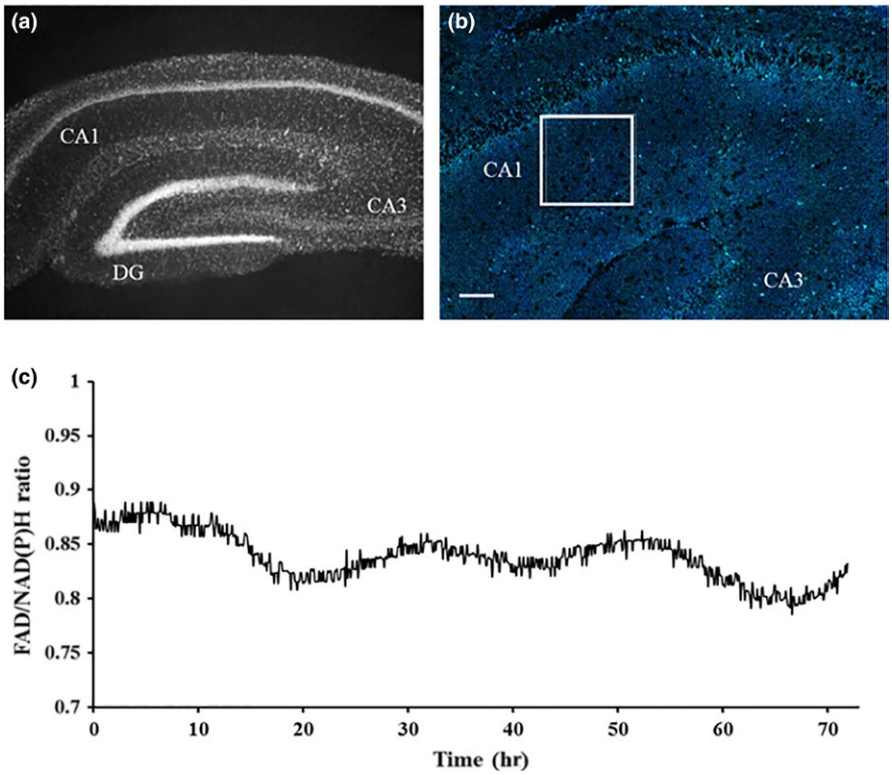

FIGURE 2 The hippocampal CA1 layer undergoes an endogenous oscillation in redox state with a ~24-hr period. (a) Excised hippocampal tissue stained with DAPI to label cell nuclei displays the tri-synaptic loop of information processing: information enters through the dentate gyrus (DG), passes through the CA3 layer, and leaves via the CA1 region. Scale bar = 500 μm. (b) Ratiometric imaging of the endogenous fluorescence of FAD/NAD(P)H was performed on the CA1 region of the live hippocampal slice. Excitation wavelength was set to 730 nm and two windows of emission at 430–500 nm and 500–550 nm were recorded simultaneously. Scale bar = 100 μm. (c) Real-time imaging of the relative redox state in the CA1 region of hippocampal brain slices revealed a near-24-hr oscillation over 72 hr. Measurement was taken from the box in (b) over this period. Ratio of FAD (500+ nm)/NAD(P)H (400+ nm) plotted against time (hr) shows an oscillation. Period (τ) = 22.75, determined by chi-square periodogram analysis. Long-term imaging of a second hippocampal slice over 72 hr recorded an oscillation over 36 hr that resembled the first, although the duration did not permit periodogram analysis

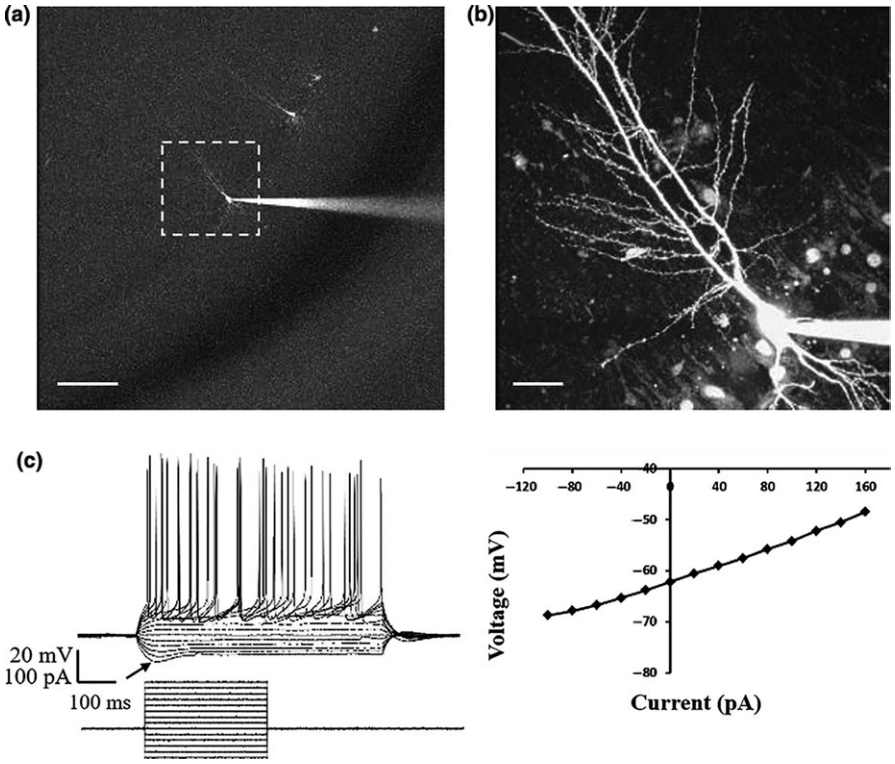

FIGURE 3 Hippocampal CA1 pyramidal neurons exhibit distinctive morphological and electrophysiological properties using dye-filling and whole-cell patch-clamp recording. (a) Multiple pyramidal neurons along the CA1 layer were filled with Alexa Fluor 488 dye. Scale bar = 100 μm. (b) Image of a single CA1 pyramidal neuron shown in the dashed box in (a) was taken on a two-photon laser-scanning microscope. Scale bar = 20 μm. (c) Voltage response of a hippocampal CA1 pyramidal neuron was measured in response to hyperpolarizing and depolarizing current pulses ranging from −100 to +160 pA with 20 pA increments. The arrow points to the depolarizing sag in response to hyperpolarizing currents, indicating the hyperpolarization-activated cation current (I_h). $n = 112$, 112 brain slices, 30 animals

~50 mV (Martina, Schultz, Ehmke, Monyer, & Jonas, 1998; McKiernan & Marrone, 2017; Routh, Johnston, Harris, & Chitwood, 2009). In addition, these neurons display a depolarizing sag in response to hyperpolarizing current pulses, indicative of the hyperpolarization-activated cation current I_h (Gasparini & DiFrancesco, 1997; Gasselin, Inglebert, & Debanne, 2015; van Welie, van Hooft, & Wadman, 2004) (Figure 3c, $n = 112$).

3.4 | Membrane excitability of CA1 pyramidal neurons oscillates over the circadian cycle

We examined membrane excitability of rat hippocampal CA1 neurons in 112 slices from 30 animals by measuring intrinsic membrane properties, including resting Vm and Rin, at 21 time points over the circadian cycle (CT 1–21) under constant conditions in vitro. Based on recordings from 112 current-clamped neurons, Vm oscillates over ~24 hr, throughout the circadian cycle. Analysis of mean Vm at six CT intervals showed that the resting Vm is significantly most hyperpolarized in subjective mid-day (CT 7: −72.73 ± 0.56 mV) and significantly most depolarized during subjective early day (CT 1: −68.29 ± 0.79 mV, $t_{106} = -4.54$, $p = 0.0002$), early night (CT 14: −69.46 ± 0.79 mV, $t_{106} = -3.34$, $p = 0.01$), and late night (CT 21: −66.06 ± 1.78 mV, $t_{106} = -3.56$, $p = 0.007$) (Figure 4, One-way ANOVA with Tukey's post-hoc test, $F_{5,106} = 6.43$, $p < 0.0001$, $n = 4$–40/CT). No statistically significant gender differences in Vm were observed (data not shown).

Additionally, Rin of the same population of cells ($n = 112$) measured from slopes of I-V curves at the beginning of recording exhibited significantly lower values at subjective late day (CT 11: 90.04 ± 9.51 MΩ) as opposed to subjective early day (CT 1: 115.27 ± 7.96 MΩ, $t_{106} = -2.03$, $p = 0.04$) and late night (CT 21:119.97 ± 13.45 MΩ, $t_{106} = -2.01$, $p = 0.04$). Similarly, Rin measured from the changes in the Vm responses to hyperpolarizing current steps, as a measure of the stability of the patch throughout the recording, showed a time-of-day change, with values significantly lower during subjective late day (CT 11: 115.22 ± 18.35 MΩ) than early night (CT 14: 167.01 ± 17.17 MΩ, $t_{106} = -2.06$, $p = 0.04$) and late night (CT 21: 172.16 ± 25.96 MΩ, $t_{106} = -1.99$, $p = 0.04$) (Figure 5c, One-way ANOVA with Tukey's post-hoc test, $F_{5,106} = 2.18$, $p = 0.03$, $n = 7$–47/CT). (Figure 5d, One-way ANOVA with Tukey's post-hoc test, $F_{5,106} = 2.48$, $p = 0.02$, $n = 7$–47/CT).

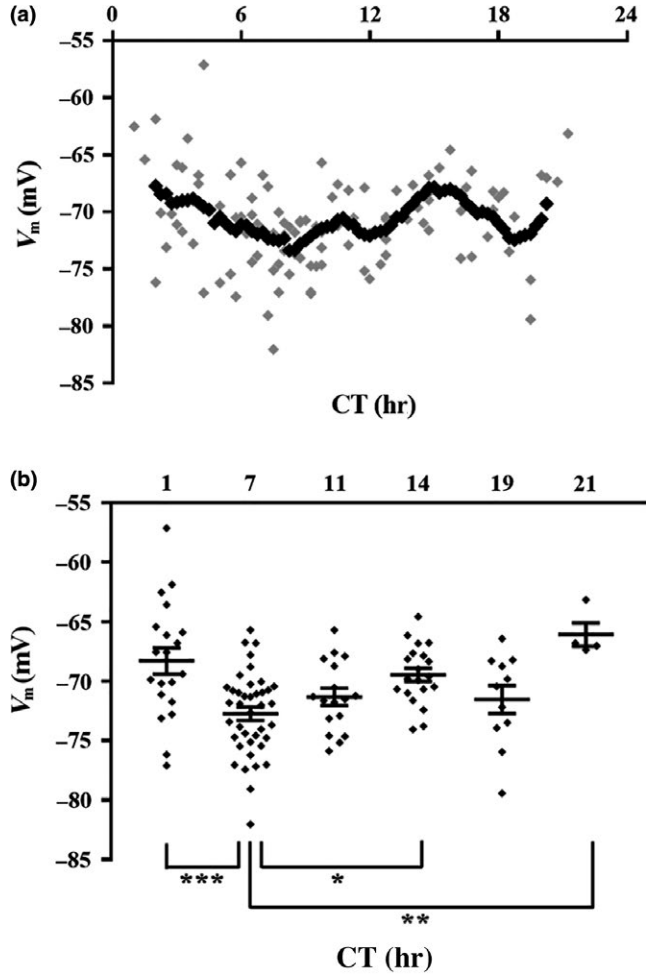

FIGURE 4 Membrane excitability of hippocampal CA1 pyramidal neurons oscillates in vitro with neurons more depolarized in subjective late night/subjective early day and significantly hyperpolarized in subjective mid-day. (a) Individual CA1 neurons (gray) and 2-hr running averages (black) exhibit oscillation in Vm assessed over 21 hr in vitro ($n = 112$ cells in 112 brain slices from 30 animals). (b) Mean Vm of CA1 neurons over six CT intervals is most hyperpolarized at CT 7 (-72.73 ± 0.56 mV) and most depolarized at CT 1 (-68.29 ± 0.79 mV, $p = 0.0002$), CT 14 (-69.46 ± 0.79 mV, $p = 0.01$), and CT 21 (-66.06 ± 1.78 mV, $p = 0.007$). One-way ANOVA; Tukey's *post-hoc* test. *$p < 0.05$, **$p < 0.01$, ***$p < 0.001$, $n = 4$–40/CT. Error bars represent SEM

3.5 | Sensitivity to glutathione-induced membrane depolarization varies over the circadian cycle in CA1 pyramidal neurons in vitro

To investigate the potential interdependency of redox state and neuronal excitability, we tested effects of pharmacological redox manipulation on Vm of hippocampal CA1 pyramidal neurons at various time points in the circadian cycle. We found that the reducing reagent, glutathione (GSH, 1 mM), depolarized Vm in a reversible manner, the magnitude of which was larger during the day (CT 7) than night (CT 14) (Figure 6a). Sensitivity to GSH-induced depolarization of membrane potential in individual CA1 pyramidal cells showed oscillations throughout the circadian cycle, with a mean depolarization of $+8.66 \pm 4.08$ mV ($n = 63$, 63 brain slices, 20 animals, CT 1–21) (Figure 6b).

Analysis of GSH-induced depolarization of membrane potential at five intervals determined that exogenous redox regulation of Vm depended upon CT. Minimal effects were seen during subjective early night (CT 14, $+5.51 \pm 0.78$ mV), whereas changes in Vm were the largest during subjective early day (CT 1: $+12.49 \pm 1.69$ mV, $t_{58} = 3.74$, $p = 0.003$), mid-day (CT 7: $+10.66 \pm 0.91$ mV, $t_{58} = 4.31$, $p = 0.0006$), and late night (CT 20: $+10.89 \pm 1.02$ mV, $t_{58} = 4.19$, $p = 0.0009$) (Figure 6c, One-way ANOVA with Tukey's *post-hoc* test, $F_{4,58} = 7.88$, $p < 0.0001$, $n = 4$–19/CT).

Shifts in Vm due to exogenous redox reagents could be associated with changes of input resistance. However, based upon the slopes of I-V curves constructed before and during GSH treatment, the reducing reagent did not cause a significant change in the input resistance of hippocampal CA1 neurons (data not shown).

3.6 | Intrinsic redox state of the hippocampus undergoes oscillation over the circadian cycle

In addition to assessing time-of-day changes in redox state, we evaluated the capacity of the hippocampus to incorporate BioGEE every 4 hr around the clock. All western blots assayed for BioGEE incorporation into tissue in brain slices are shown in Supporting Information Figure S2. Quantification of western blots showed that tissue-level glutathiolation was lowest at CT 14 ($28.06 \pm 3.6\%$), indicating a relatively reduced state at subjective early night, and highest between CT 6 ($84.74 \pm 8.9\%$, $t_{18} = 5.12$, $p = 0.0009$) and CT 10 ($90.15 \pm 4.57\%$, $t_{18} = 5.61$, $p = 0.0003$), indicating a relatively oxidized state during the subjective day. (Figure 6d, One-way ANOVA with Tukey's post-hoc test, $F_{5,18} = 8.66$, $p = 0.0003$, $n = 4$/CT).

4 | DISCUSSION

There have long been reports of the time-of-day effects on memory formation (Chaudhury et al., 2005; Fekete et al., 1985; Holloway & Wansley, 1973; Tapp & Holloway, 1981). Although the SCN does not directly innervate the hippocampus, information about the time-of-day can reach the hippocampus through indirect synaptic inputs (Wyss, Swanson, & Cowan, 1979). More recent studies have revealed circadian oscillations of clock gene expression as well as components of signaling cascades, such as the cAMP-MAPK-CREB pathway that regulates both circadian rhythms

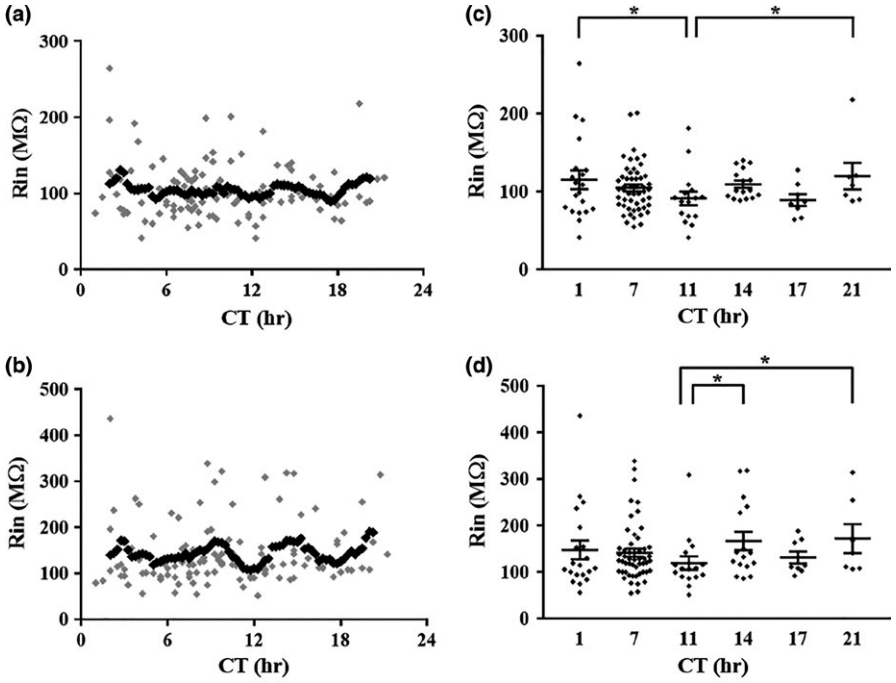

FIGURE 5 Membrane input resistance of hippocampal CA1 pyramidal neurons undergoes a time-of-day change in vitro. (a) Individual CA1 neurons (gray) and 2-hr running averages (black) exhibit a difference in Rin measured from I-V curves constructed by current steps from −100 to +200 pA with 20 pA increments and a 600 ms duration ($n = 112$). This is a measure of the initial resistance of the cell at the beginning of the recording. (b) Individual CA1 neurons (gray) and 2-hr running averages (black) exhibit a change in Rin measured from hyperpolarizing current steps which assesses the health of the neuron and the stability of the patch throughout the recording ($n = 112$). (c) Average Rin measured from the slope of I-V curves at six CT intervals has significantly lower input resistances at CT 11 (90.04 ± 9.51 MΩ) vs. CT 1 (115.27 ± 7.96 MΩ, $p = 0.04$) and CT 21 (119.97 ± 13.45 MΩ, $p = 0.04$). (d) Average Rin from hyperpolarizing current steps at six CT intervals show significantly lower input resistances at CT 11 (115.22 ± 18.35 MΩ) vs. CT 14 (167.01 ± 17.17 MΩ, $p = 0.04$) and CT 21 (172.16 ± 25.96 MΩ, $p = 0.04$). One-way ANOVA; Tukey's post-hoc test. *$p < 0.05$, $n = 7$–47/CT. Error bars represent SEM

and memory formation (Butcher, Dziema, Collamore, Burgoon, & Obrietan, 2002; Eckel-Mahan & Storm, 2009; Eckel-Mahan et al., 2008; Iyer, Wang, & Gillette, 2014; Kandel, 2012; Obrietan, Impey, Smith, Athos, & Storm, 1999; Obrietan, Impey, & Storm, 1998; Tischkau, Mitchell, Tyan, Buchanan, & Gillette, 2003). Here, we investigate whether another property is shared between the SCN and hippocampus: oscillation in redox state over the circadian cycle.

Using long-term ratiometric imaging of specific redox cofactors, we show, for the first time, an oscillation of redox state with a ~24 hr period in the CA1 layer of a rat hippocampus (Figure 2). This redox oscillation is sustained in an isolated hippocampal brain slice for at least 3 days. Phasing of the redox rhythm in the hippocampal CA1 layer is inverted from that of the SCN, with subjective night being most reduced and subjective day being most oxidized (Figure 1). Significantly, this aligns with the local expression patterns of circadian clock genes, which also are in anti-phase between hippocampus and SCN (Wang et al., 2009).

Although there have been no previous reports of a near-24-hr redox rhythm in the hippocampus, there is evidence for daily oscillations in its antioxidant enzyme activity. Glutathione peroxidase (GSH-Px) and catalase activity levels show diurnal rhythms in samples from the rat hippocampus (Fonzo et al., 2011). Furthermore, the inhibitory phosphorylation of the redox-sensitive enzyme, glycogen synthase kinase 3-beta (GSK3β), exhibits an endogenous day-night rhythm in the hippocampal CA1 region that persists in constant darkness. GSK3 is not only necessary for regulation of molecular clock genes in the hippocampus but is also crucial for maintenance of day-night differences in the LTP in the CA1 region (Besing et al., 2017). Taken together, these data support our finding of a temporal pattern of redox activity in the hippocampus.

Another major finding of this study is that the membrane excitability of CA1 pyramidal neurons of the rat hippocampus displays oscillations (Figure 4). This observation is of particular importance as we chose to focus only on the primary hippocampal projection neurons. These neurons carry information processed by the hippocampus back to the entorhinal cortex for transmission to other brain regions (Andersen, Bliss, Lomo, Olsen, & Skrede, 1969). During subjective day (CT 7), a time of rest in the nocturnal rodent, Vm in these neurons is significantly more hyperpolarized, whereas during subjective night (CT 14), the active period, the resting Vm is

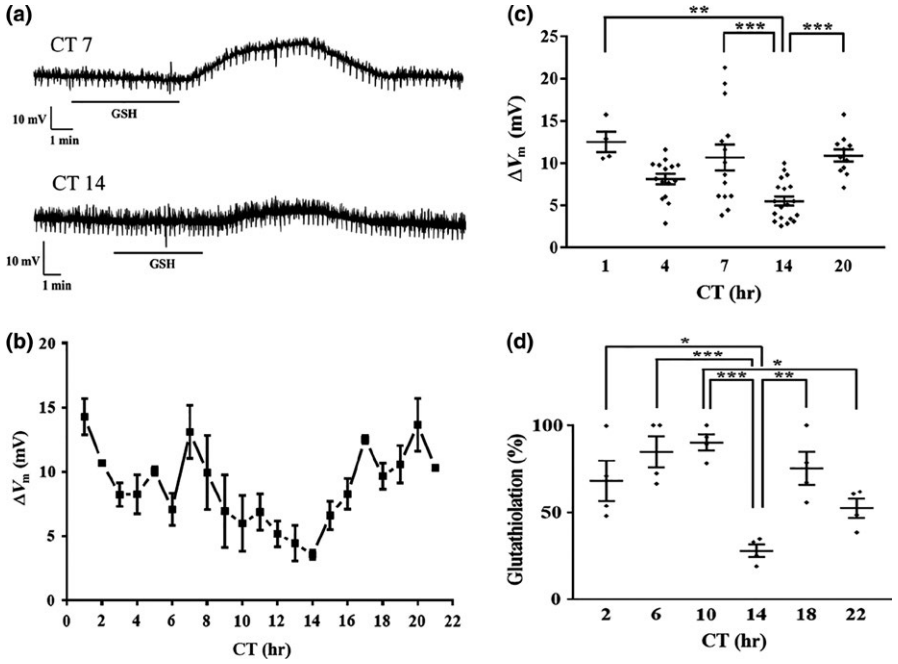

FIGURE 6 Redox-induced changes in membrane excitability of hippocampal CA1 pyramidal neurons align with the endogenous redox oscillation of the hippocampus. (a) Glutathione (GSH, 1 mM, 5 min) produced a rapid, reversible membrane depolarization from the baseline with magnitudes significantly larger during mid-day (CT 7) compared to the early night (CT 14). (b) GSH-induced depolarization in 63 individual CA1 pyramidal neurons showed oscillation over 21 hr throughout the circadian cycle (n = 1–6/CT, total of 63 brain slices, 20 animals). (c) GSH-induced depolarization of Vm in CA1 neurons at five CT groups showed the smallest ΔVm at CT 14 (5.51 ± 0.78 mV) and the largest ΔVm at CT 1 (12.49 ± 1.69 mV, $p = 0.003$), CT 7 (10.66 ± 0.91 mV, $p = 0.0006$), and CT 20 (10.89 ± 1.02 mV, $p = 0.0009$). One-way ANOVA; Tukey's *post-hoc* test. $^{**}p < 0.01$, $^{***}p < 0.001$, n = 4–19/CT. (d) To assess the hippocampal intrinsic redox oscillation, quantification of all western blots assayed for BioGEE incorporation was performed. Tissue-level glutathiolation was lowest at CT 14 (28.06 ± 3.6%) and highest at CT 2 (68.12 ± 11.61%, $p = 0.02$), CT 6 (84.74 ± 8.9%, $p = 0.0009$), CT 10 (90.15 ± 4.57%, $p = 0.0003$), and CT 18 (75.33 ± 9.43%, $p = 0.005$). This indicates that the hippocampus is most reduced at CT 14, which aligns with the smallest GSH-induced Vm change at this time point. One-way ANOVA; Tukey's *post-hoc* test. $^{*}p < 0.05$, $^{**}p < 0.01$, $^{***}p < 0.001$, $n = 4$. Error bars represent SEM

significantly more depolarized. This is ~180° out-of-phase with SCN membrane potential changes (Wang et al., 2012). Additionally, we found that hippocampal CA1 pyramidal neurons are significantly more depolarized during subjective early day when night transitions to day (CT 1) compared to the mid-day (CT 7), which again is the opposite of the SCN (Wang et al., 2012).

The changes in input resistance are associated with shifts in Vm of current-clamped hippocampal CA1 neurons (Figure 5). The CA1 pyramidal neurons have significantly higher Rin levels in early night (CT 14) and during late night and subjective early day (CT 21 and CT 1), which coincides with the Vm being most depolarized. The same relationship between the Vm and Rin was reported in the current-clamped SCN neurons, where the higher Rin levels during the subjective mid-day matched with the Vm being most depolarized, and significantly lower Rin levels in early night coincided with Vm being more hyperpolarized (Wang et al., 2012). These findings are of particular interest as, in the hippocampus, the peak expression level of the *Per2* clock gene was reported in the late night/early morning (between CT 23 and CT 2) (Wang et al., 2009). This aligns with our observed higher Rin levels of the subjective late night to subjective early day. Conversely, a trough of *Per2* expression was found in the late day (Wang et al., 2009), which matches our observed lower Rin levels in the late day (CT 11).

Exposure to the reducing reagent, GSH, depolarized the Vm of hippocampal CA1 pyramidal neurons in a reversible manner. This change also was observed in the SCN neurons. As shown previously, this redox reagent-induced change has the same amplitude as the observed endogenous redox oscillation (Wang et al., 2012). Based on the opposite oscillation in the Vm of hippocampal vs. SCN neurons, the exogenous redox regulation of Vm was expected to be anti-phase to the SCN, as well. As predicted, we observed minimal GSH-induced depolarization of Vm in hippocampal CA1 neurons in subjective early night and maximal effects during early day, mid-day, and late night (Figure 6), which are opposite of the changes in the SCN (Wang et al., 2012). Thus, the GSH-induced changes in Vm are CT-dependent and in anti-phase in the SCN vs. hippocampal CA1 neurons.

To determine the redox level in the hippocampal tissue, glutathiolation was evaluated at various time points throughout the circadian cycle of hippocampal brain slices.

Glutathiolation reports the capacity of proteins to incorporate reduced GSH, which binds to available reactive cysteine side chains (Hill & Bhatnagar, 2012). In the hippocampus, higher levels of tissue-level glutathiolation are observed during the subjective day, indicating a relatively oxidized state, whereas lower levels are found during early night, indicating a relatively reduced state (Figure 6d). This finding in the hippocampus is opposite of the glutathiolation pattern in the SCN (Wang et al., 2012). Comparison of these results with changes in Vm in hippocampal CA1 pyramidal neurons indicates a rhythm in neuronal membrane properties with the Vm being more hyperpolarized during the subjective day when the hippocampus is more oxidized and more depolarized in the subjective night when the hippocampus is more reduced. This change is the opposite of that in the SCN (Wang et al., 2012) and agrees with our findings that the magnitude of the GSH-induced depolarization is significantly larger during the day than nighttime. These data show not only a tissue-level redox oscillation in the hippocampus but also that redox rhythm can regulate membrane excitability of neurons. As the redox potential of various redox couples differs among cellular compartments (Go & Jones, 2008), it will be important to determine the redox changes in specific cellular compartments, such as the cytosol, the mitochondria, or the nucleus.

An unanswered question is whether these hippocampal oscillations in neural activity, clock gene expression, and redox state are dependent on the SCN. There is evidence that cycling elements in the hippocampus may depend on a functional SCN and the core molecular clock. Per2::LUC bioluminescence rhythms persist for several days in the hippocampal slice without input from the SCN. However, such input may be required to maintain the synchronization and amplitude of cell-based rhythms (Wang et al., 2009). The oscillation of *Per2* in the dentate gyrus can be abolished by SCN lesions that also abolish locomotor activity rhythm (Lamont, Robinson, Stewart, & Amir, 2005). Cycling of MAPK and adenylyl cyclase activity in the hippocampus appears to be SCN-dependent, as ablation of the SCN eliminates the diurnal oscillation of both (Phan, Chan, Sindreu, Eckel-Mahan, & Storm, 2011). Furthermore, the hippocampus of *Bmal1*$^{-/-}$ mice does not exhibit a diurnal rhythm in MAPK activity and cAMP levels (Wardlaw, Phan, Saraf, Chen, & Storm, 2014). Evaluating animals with clock gene deletions or SCN ablation for the presence of hippocampal redox oscillation is an important subject of future studies.

In conclusion, both neuronal membrane excitability and redox state exhibit oscillations in the rat hippocampal CA1 pyramidal neurons around the circadian cycle. Both patterns are ~180° out-of-phase with those reported previously in the SCN neurons (Wang et al., 2012). This study was limited to recording at only 21 time points throughout the circadian cycle because it is difficult to keep acute hippocampal slices alive for more than 8–9 hr in the open brain slice chamber used for patch recordings. The slicing process could potentially damage the numerous lengthy projections extending from CA1 pyramidal neurons to other brain regions (Arszovski, Borhegyi, & Klausberger, 2014). This has been shown not to be a problem in the SCN brain slices, where efferent projections are relatively short and limited to within the hypothalamic region (Campos, Cruz-Rizzolo, Watanabe, Pinato, & Nogueira, 2014).

The circadian rhythm of neuronal excitability in the hippocampus is poised to be a powerful regulator with key roles in modulating long-term potentiation, memory acquisition, and recall of learned behaviors (Chaudhury et al., 2005; Ruby et al., 2008). Here, we provide evidence of a non-transcriptional mechanism of interdependency between the metabolic state and electrical activity in the pyramidal cells of the CA1 layer over the day-night cycle. Our study suggests that changes in the redox state may be an intrinsic regulator of change in pyramidal cell excitability, rather than a consequence of it. This study further bridges the gap between metabolic state and neuronal activity at the local cellular level to the global system of physiology and behavior. These insights enrich understanding of circadian-based functions and potential dysfunctions in the hippocampus and enable testable predictions about the regulation of hippocampus-specific functions, such as synaptic plasticity, memory formation, and age-related cognitive deficits.

ACKNOWLEDGEMENTS

The authors thank Jennifer W. Mitchell for assistance in brain slice preparation, insight on figure preparation, and review of the manuscript, and Ann C. Benefiel for help with manuscript submission. We acknowledge Kathleen Louis of Michigan State University for assistance with acquiring images used in Figure 3a,b. We also thank Ian Bothwell, University of Illinois, for assistance with the graphical abstract. This study was supported by funding from the Beckman Institute Graduate Fellows Program at the University of Illinois, the Medical Scholars Program at the University of Illinois, the National Institutes of Health (U01 MH 109062), and the National Science Foundation (IGERT CMMB 0965918, CBET STC 0939511, and IOS 1354913). These sources of funding had no involvement in the study design, data collection, analysis, and interpretation, writing of the report, or in the decision to submit the paper for publication. This work was conducted in part at the Beckman Institute for Advanced Science and Technology at the University of Illinois at Urbana-Champaign.

CONFLICT OF INTEREST

The authors have no conflict of interest to declare.

DATA ACCESSIBILITY

All primary data are available at Figshares.

AUTHORS' CONTRIBUTIONS

Ghazal Naseri Kouzehgarani and Mia Y. Bothwell contributed equally to the experimental studies presented in the manuscript. All authors read, revised, and approved the final manuscript.

ORCID

Martha U. Gillette https://orcid.org/0000-0003-3645-2626

REFERENCES

Abe, M., Herzog, E. D., Yamazaki, S., Straume, M., Tei, H., Sakaki, Y., … Block, G. D. (2002). Circadian rhythms in isolated brain regions. *Journal of Neuroscience*, *22*, 350–356. https://doi.org/10.1523/JNEUROSCI.22-01-00350.2002

Andersen, P., Bliss, T. V., Lomo, T., Olsen, L. I., & Skrede, K. K. (1969). Lamellar organization of hippocampal excitatory pathways. *Acta Physiologica Scandinavica*, *76*, 4A–5A.

Arszovski, A., Borhegyi, Z., & Klausberger, T. (2014). Three axonal projection routes of individual pyramidal cells in the ventral CA1 hippocampus. *Frontiers in Neuroanatomy*, *8*, 53.

Bass, J., & Takahashi, J. S. (2010). Circadian integration of metabolism and energetics. *Science*, *330*, 1349–1354. https://doi.org/10.1126/science.1195027

Besing, R. C., Rogers, C. O., Paul, J. R., Hablitz, L. M., Johnson, R. L., McMahon, L. L., & Gamble, K. L. (2017). GSK3 activity regulates rhythms in hippocampal clock gene expression and synaptic plasticity. *Hippocampus*, *27*, 890–898. https://doi.org/10.1002/hipo.22739

Bothwell, M. Y., & Gillette, M. U. (2018). Circadian redox rhythms in the regulation of neuronal excitability. *Free Radical Biology & Medicine*, *119*, 45–55. https://doi.org/10.1016/j.freeradbiomed.2018.01.025

Butcher, G. Q., Dziema, H., Collamore, M., Burgoon, P. W., & Obrietan, K. (2002). The p42/44 mitogen-activated protein kinase pathway couples photic input to circadian clock entrainment. *Journal of Biological Chemistry*, *277*, 29519–29525. https://doi.org/10.1074/jbc.M203301200

Campos, L. M., Cruz-Rizzolo, R. J., Watanabe, I. S., Pinato, L., & Nogueira, M. I. (2014). Efferent projections of the suprachiasmatic nucleus based on the distribution of vasoactive intestinal peptide (VIP) and arginine vasopressin (AVP) immunoreactive fibers in the hypothalamus of *Sapajus apella*. *Journal of Chemical Neuroanatomy*, *57–58*, 42–53. https://doi.org/10.1016/j.jchemneu.2014.03.004

Chaudhury, D., & Colwell, C. S. (2002). Circadian modulation of learning and memory in fear-conditioned mice. *Behavioral Brain Research*, *133*, 95–108. https://doi.org/10.1016/S0166-4328(01)00471-5

Chaudhury, D., Wang, L. M., & Colwell, C. S. (2005). Circadian regulation of hippocampal long-term potentiation. *Journal of Biological Rhythms*, *28*, 225–236. https://doi.org/10.1177/0748730405276352

Cho, K., Ennaceur, A., Cole, J. C., & Suh, C. K. (2000). Chronic jet lag produces cognitive deficits. *Journal of Neuroscience*, *20*, RC66. https://doi.org/10.1523/JNEUROSCI.20-06-j0005.2000

Dröge, W. (2002). Free radicals in the physiological control of cell function. *Physiological Reviews*, *82*, 47–95. https://doi.org/10.1152/physrev.00018.2001

Eckel-Mahan, K. L., Phan, T., Han, S., Wang, H., Chan, G. C., Scheiner, Z. S., & Storm, D. R. (2008). Circadian oscillation of hippocampal MAPK activity and cAMP: Implications for memory persistence. *Nature Neuroscience*, *11*, 1074–1082. https://doi.org/10.1038/nn.2174

Eckel-Mahan, K. L., & Storm, D. R. (2009). Circadian rhythms and memory: Not so simple as cogs and gears. *EMBO Reports*, *10*, 584–591. https://doi.org/10.1038/embor.2009.123

Feillet, C. A., Mendoza, J., Albrecht, U., Pévet, P., & Challet, E. (2008). Forebrain oscillators ticking with different clock hands. *Molecular and Cellular Neurosciences*, *37*, 209–221. https://doi.org/10.1016/j.mcn.2007.09.010

Fekete, M., van Ree, J. M., Niesink, R. J., & de Wied, D. (1985). Disrupting circadian rhythms in rats induces retrograde amnesia. *Physiology & Behavior*, *34*, 883–887. https://doi.org/10.1016/0031-9384(85)90008-3

Fonzo, L. S., Golini, R. S., Delgado, S. M., Ponce, I. T., Bonomi, M. R., Rezza, I. G., … Anzulovich, A. C. (2011). Temporal patterns of lipoperoxidation and antioxidant enzymes are modified in the hippocampus of vitamin A-deficient rats. *Hippocampus*, *19*, 869–880.

Gasparini, S., & DiFrancesco, D. (1997). Action of the hyperpolarization-activated current (Ih) blocker ZD 7288 in hippocampal CA1 neurons. *Pflugers Archiv European Journal of Physiology*, *435*, 99–106. https://doi.org/10.1007/s004240050488

Gasselin, C., Inglebert, Y., & Debanne, D. (2015). Homeostatic regulation of h-conductance controls intrinsic excitability and stabilizes the threshold for synaptic modification in CA1 neurons. *Journal of Physiology*, *593*, 4855–4869. https://doi.org/10.1113/JP271369

Georgakoudi, I., & Quinn, K. P. (2012). Optical imaging using endogenous contrast to assess metabolic state. *Annual Review of Biomedical Engineering*, *14*, 351–367. https://doi.org/10.1146/annurev-bioeng-071811-150108

Gillette, M. U. (1985). Preparation of brain slices from the suprachiasmatic nuclei of rat can reset the circadian clock. *Journal of Physiology*, *369*, 55P.

Gillette, M. U., & Wang, T. A. (2014). Brain oscillators and redox mechanisms in mammals. *Antioxidants & Redox*, *20*, 2955–2965. https://doi.org/10.1089/ars.2013.5598

Go, Y. M., & Jones, D. P. (2008). Redox compartmentalization in eukaryotic cells. *Biochimica et Biophysica Acta*, *1780*, 1273–1290. https://doi.org/10.1016/j.bbagen.2008.01.011

Granados-Fuentes, D., Prolo, L. M., Abraham, U., & Herzog, E. D. (2004). The suprachiasmatic nucleus entrains, but does not sustain, Circadian rhythmicity in the olfactory bulb. *Journal of Neuroscience*, *24*, 615–619. https://doi.org/10.1523/JNEUROSCI.4002-03.2004

Green, C. B., Takahashi, J. S., & Bass, J. (2008). The meter of metabolism. *Cell*, *134*, 728–742. https://doi.org/10.1016/j.cell.2008.08.022

Griffiths, H. R., Gao, D., & Pararasa, C. (2017). Redox regulation in metabolic programming and inflammation. *Redox Biology*, *12*, 50–57. https://doi.org/10.1016/j.redox.2017.01.023

Guilding, C., & Piggins, H. D. (2007). Challenging the omnipotence of the suprachiasmatic timekeeper: Are circadian oscillators present throughout the mammalian brain? *European Journal of Neuroscience*, *25*, 3195–3216. https://doi.org/10.1111/j.1460-9568.2007.05581.x

Harris, K. M., & Teyler, T. J. (1983). Age differences in a circadian influence on hippocampal LTP. *Brain Research*, *261*, 69–73. https://doi.org/10.1016/0006-8993(83)91284-2

Hill, B. G., & Bhatnagar, A. (2012). Protein S-glutathiolation: Redox-sensitive regulation of protein function. *Journal of Molecular and Cellular Cardiology*, *52*, 559–567. https://doi.org/10.1016/j.yjmcc.2011.07.009

Holloway, F. A., & Wansley, R. A. (1973). Multiple retention deficits at periodic intervals after active and passive avoidance learning. *Behavioral Biology*, *9*, 1–14. https://doi.org/10.1016/S0091-6773(73)80164-6

Iyer, R., Wang, T. A., & Gillette, M. U. (2014). Circadian gating of neuronal functionality: A basis for iterative metaplasticity. *Frontiers in Systems Neuroscience*, *8*, 164.

Kandel, E. R. (2012). The molecular biology of memory: cAMP, PKA, CRE, CREB-1, CREB-2, and CPEB. *Molecular Brain*, *5*, 14. https://doi.org/10.1186/1756-6606-5-14

Lamont, E. W., Robinson, B., Stewart, J., & Amir, S. (2005). The central and basolateral nuclei of the amygdala exhibit opposite diurnal rhythms of expression of the clock protein Period2. *Proceedings of the National Academy of Sciences of the United States of America*, *102*, 4180–4184. https://doi.org/10.1073/pnas.0500901102

Martina, M., Schultz, J. H., Ehmke, H., Monyer, H., & Jonas, P. (1998). Functional and molecular differences between voltage-gated K+ channels of fast-spiking interneurons and pyramidal neurons of rat hippocampus. *Journal of Neuroscience*, *18*, 8111–8125. https://doi.org/10.1523/JNEUROSCI.18-20-08111.1998

McKiernan, E. C., & Marrone, D. F. (2017). CA1 pyramidal cells have diverse biophysical properties, affected by development, experience, and aging. *PeerJ.*, *5*, e3836. https://doi.org/10.7717/peerj.3836

Obrietan, K., Impey, S., Smith, D., Athos, J., & Storm, D. R. (1999). Circadian regulation of cAMP response element-mediated gene expression in the suprachiasmatic nuclei. *Journal of Biological Chemistry*, *274*, 17748–17756. https://doi.org/10.1074/jbc.274.25.17748

Obrietan, K., Impey, S., & Storm, D. R. (1998). Light and circadian rhythmicity regulate MAP kinase activation in the suprachiasmatic nuclei. *Nature Neuroscience*, *1*, 693–700. https://doi.org/10.1038/3695

Phan, T. H., Chan, G. C., Sindreu, C. B., Eckel-Mahan, K. L., & Storm, D. R. (2011). The diurnal oscillation of MAP (mitogen-activated protein) kinase and adenylyl cyclase activities in the hippocampus depends on the suprachiasmatic Nucleus. *Journal of Neuroscience*, *31*, 10640–10647. https://doi.org/10.1523/JNEUROSCI.6535-10.2011

Routh, B. N., Johnston, D., Harris, K., & Chitwood, R. A. (2009). Anatomical and electrophysiological comparison of CA1 pyramidal neurons of the rat and mouse. *Journal of Neurophysiology*, *102*, 2288–2302. https://doi.org/10.1152/jn.00082.2009

Ruby, N. F., Hwang, C. E., Wessells, C., Fernandez, F., Zhang, P., Sapolsky, R., & Heller, H. C. (2008). Hippocampal-dependent learning requires a functional circadian system. *Proceedings of the National Academy of Sciences of the United States of America*, *105*, 15593–15598. https://doi.org/10.1073/pnas.0808259105

Rutter, J., Reick, M., & McKnight, S. L. (2002). Metabolism and the control of circadian rhythms. *Annual Review of Biochemistry*, *71*, 307–331. https://doi.org/10.1146/annurev.biochem.71.090501.142857

Schafer, F. Q., & Buettner, G. R. (2001). Redox environment of the cell as viewed through the redox state of the glutathione disulfide/glutathione couple. *Free Radical Biology and Medicine*, *30*, 1191–1212. https://doi.org/10.1016/S0891-5849(01)00480-4

Stephan, F. K., & Kovacevic, N. S. (1978). Multiple retention deficit in passive avoidance in rats is eliminated by suprachiasmatic lesions. *Behavioral Biology*, *22*, 456–462. https://doi.org/10.1016/S0091-6773(78)92565-8

Tapp, W. N., & Holloway, F. A. (1981). Phase shifting circadian rhythms produces retrograde amnesia. *Science*, *211*, 1056–1058. https://doi.org/10.1126/science.7193351

Tischkau, S. A., Mitchell, J. W., Tyan, S. H., Buchanan, G. F., & Gillette, M. U. (2003). Ca2+/cAMP response element-binding protein (CREB)-dependent activation of Per1 is required for light-induced signaling in the suprachiasmatic nucleus circadian clock. *Journal of Biological Chemistry*, *278*, 718–723. https://doi.org/10.1074/jbc.M209241200

Wakamatsu, H., Yoshinobu, Y., Aida, R., Moriya, T., Akiyama, M., & Shibata, S. (2001). Restricted-feeding-induced anticipatory activity rhythm is associated with a phase-shift of the expression of mPer1 and mPer2 mRNA in the cerebral cortex and hippocampus but not in the suprachiasmatic nucleus of mice. *European Journal of Neuroscience*, *13*, 1190–1196. https://doi.org/10.1046/j.0953-816x.2001.01483.x

Wang, L. M., Dragich, J. M., Kudo, T., Odom, I. H., Welsh, D. K., O'Dell, T. J., & Colwell, C. S. (2009). Expression of the circadian clock gene Period2 in the hippocampus: Possible implications for synaptic plasticity and learned behaviour. *ASN Neuro*, *1*, 139–152.

Wang, T. A., Yu, Y. V., Govindaiah, G., Ye, X., Artinian, L., Coleman, T. P., … Gillette, M. U. (2012). Circadian rhythm of redox state regulates excitability in suprachiasmatic nucleus neurons. *Science*, *337*, 839–842. https://doi.org/10.1126/science.1222826

Wardlaw, S. M., Phan, T. X., Saraf, A., Chen, X., & Storm, D. R. (2014). Genetic disruption of the core circadian clock impairs hippocampus-dependent memory. *Learning & Memory*, *21*, 417–423. https://doi.org/10.1101/lm.035451.114

van Welie, I., van Hooft, J. A., & Wadman, W. J. (2004). Homeostatic scaling of neuronal excitability by synaptic modulation of somatic hyperpolarization-activated Ih channels. *Proceedings of the National Academy of Sciences of the United States of America*, *101*, 5123–5128. https://doi.org/10.1073/pnas.0307711101

Wright, K. P. Jr, Hull, J. T., Hughes, R. J., Ronda, J. M., & Czeisler, C. A. (2006). Sleep and wakefulness out of phase with internal biological time impairs learning in humans. *Journal of Cognitive Neuroscience*, *18*, 508–521. https://doi.org/10.1162/jocn.2006.18.4.508

Wyss, J. M., Swanson, L. W., & Cowan, W. M. (1979). A study of subcortical afferents to the hippocampal formation in the rat. *Neuroscience*, *4*, 463–476. https://doi.org/10.1016/0306-4522(79)90124-6

SUPPORTING INFORMATION

Additional supporting information may be found online in the Supporting Information section at the end of the article.

How to cite this article: Naseri Kouzehgarani G, Bothwell MY, Gillette MU. Circadian rhythm of redox state regulates membrane excitability in hippocampal CA1 neurons. *Eur J Neurosci*. 2019;00:1–13. https://doi.org/10.1111/ejn.14334